

Electrical characteristics and conductivity mechanism of self-sensing asphalt concrete

Yuanyuan Li^a, Bowen Hu^a, Yangming Gao^{b,*}, Jianlin Feng^a, Patryk Kot^b

^a School of Civil Engineering and Architecture, Wuhan Institute of Technology, Wuhan 430205, Hubei, China

^b Built Environment and Sustainable Technologies (BEST) Research Institute, Liverpool John Moores University, Liverpool L3 3AF, United Kingdom

ARTICLE INFO

Keywords:

Self-sensing asphalt concrete
Sensing mechanism
Volume parameters
Electrical properties
Mechanical property

ABSTRACT

The existing conductive asphalt concrete is not suitable for self-sensing of asphalt concrete structural damage. In order to realize the perception of electrical signals on the structural damage of asphalt pavement, a self-sensing asphalt concrete is designed, and the relationship between condition change and resistance change of asphalt pavement is established by adding multi-conductive phase materials to ordinary asphalt concrete. The influence of different amounts of conductive additives on the volumetric parameters, electrical properties, and mechanical properties of asphalt concrete has been studied, the influence of volume parameter changes on the electrical properties and variability of conductive asphalt concrete was clarified, and the correlation analysis between volume of air voids (VV) and resistivity has been established. Nano-CT scanning, the distribution of conductive phase materials in asphalt concrete was characterized, and its long-short synergistic conduction mechanism was revealed, which provided a theoretical basis for the application of self-sensing asphalt concrete. Results indicate that the failure spacing of conductive particles of single-doped graphite is 2 μm , and the volume content of graphite should not be less than 0.68% to have weak conductivity. Considering the volume parameters, electrical properties and mechanical properties of asphalt concrete, the composite modification method of graphite and steel fiber is proposed, the recommended graphite content of conductive phase material is 0.68%, and the content of steel fiber is 0.9–1.1%. The internal structure failure of asphalt concrete is mainly manifested in the change of volume of air voids (VV), the electrical properties of conductive asphalt concrete show a negative correlation with the VV of concrete, and the change of resistivity of asphalt concrete can be used to predict the damage state inside the pavement structure.

1. Introduction

Asphalt pavement, as an important part of transportation infrastructure, plays a significant role in the development of the global economy and society [1,2]. In recent years, due to the continuous increase of traffic volume, the traffic load of asphalt pavement is "overloaded", and under the action of long-term temperature, humidity, ultraviolet, and other complex factors, the service properties of asphalt pavement deteriorated rapidly and the service level is significantly reduced [3,4]. The development of asphalt pavement distresses and the reduction of service level is not linear change characteristics, and the preventive maintenance of pavement distresses at the appropriate time has significant technical and economic benefits [5]. Self-monitoring of structural health (SHM), due to real-time sensing and evaluation of structural damage status, has been widely used in aerospace, bridge

engineering and mechanical engineering [6,7]. Endowing the asphalt pavement with the self-sensing function of distress is of great significance for early distress detection and the improvement of maintenance decision-making. The self-sensing of asphalt concrete enables timely understanding of the structural health status when early distress appears in asphalt roads, offering scientific guidance for maintenance, implementing corresponding reinforcement measures in a timely manner before permanent damage occurs, restoring its normal service level, reducing maintenance costs, extending the service life of the structure, and avoiding large-scale remodeling and treatment. Therefore, research on self-sensing asphalt concrete has significant economic and social benefits.

Relevant technical measures have been applied to monitor the distressing development of asphalt pavements, including real-time monitoring of road service status using sensors, timing pavement sampling

* Corresponding author.

E-mail address: y.gao@ljmu.ac.uk (Y. Gao).

<https://doi.org/10.1016/j.conbuildmat.2024.135236>

Received 15 September 2023; Received in revised form 25 January 2024; Accepted 27 January 2024

Available online 3 February 2024

0950-0618/© 2024 The Author(s). Published by Elsevier Ltd. This is an open access article under the CC BY-NC-ND license (<http://creativecommons.org/licenses/by-nc-nd/4.0/>).

detection, etc [8]. The road structure was monitored and analyzed using the fiber Bragg grating sensor (FBG) [9,10], resistance strain gauge, and embedded vibrating wire strain gauge [11]. However, most of the conventional sensors are easily damaged at the initial stage of embedding or the road surface in service has the disadvantages of poor durability and low survival rate [12], and the sensor embedded in the road surface may damage the road surface structure to a certain extent [13]. Pavement damage detection technology can be divided into three categories as a whole: (1) pavement timing sampling detection, that is, the use of artificial field sampling detection of pavement structure; (2) the digital image detection technology to detect road surface cracks[14]; and (3) the laser displacement detection technology for the purpose of detecting pavement deformations [15]. However, sampling monitoring requires a large amount of work and data acquisition efficiency is low, requiring a large number of samples, which is a loss detection method [16]; UAV (unmanned aerial vehicle), computer vision and other image-based distress detection methods can only detect the surface state of the structure [17,18]; Ground penetrating radar needs additional tractor traction equipment, and the detection timing needs artificial judgment, which is only instantaneous monitoring and does not have real-time monitoring [19]. In this sense, how to develop a road detection and data processing method suitable for a variety of working conditions, real-time monitoring of the status of the road structure, and achieving high-efficiency and intelligent road detection is the focus of the development of road detection technology in the future [18]. However, self-sensing roads can achieve real-time nondestructive testing of pavement structures without human participation, with significant technical advantages, which deserve attention and research.

With the development of advanced materials and the improvement of monitoring sensing methods, conductive phase materials have significant advantages of self-sensing function in engineering structure monitoring [19]. The conductive phase material is added into that cement concrete, so that the concrete has the conductive property, and the pavement state is judged in real-time through the change of the electrical property in the service process. Banthia [20] studied the resistivity characteristics of different carbon fiber and steel fiber reinforced cement and found that the fiber can effectively enhance the conductivity of concrete. Chung et al. [21–23] studied the relationship between the resistivity changes of carbon fiber and steel fiber reinforced silicon and the loading, and found that they have a certain approximate proportion relationship, that is to say, the fiber-reinforced cement-based composite material has the self-diagnosis ability of stress and strain, and the partial irreversibility of the resistivity changes indicates that the resistivity changes can reflect the damage of the material structure. Asphalt concrete does not have conductive properties in nature, but can be imparted with conductive properties by the addition of conductive phase materials (graphite, carbon black, carbon fiber, etc.) [24–26]. The conductive concrete is adopted to establish the correlation between the properties changes of the structural self-diagnosis asphalt pavement and the electrical properties [5], the pavement damage state is judged through the electrical properties attenuation during service, and the health condition of the pavement structure is monitored all the time to determine the optimal pavement maintenance timing [27]. In recent years, the research and application of conductive asphalt concrete are shown in Table 1. The conductivity of the conductive asphalt concrete is proportional to the volume of the conductive filler or fiber [28], and the conductive phase material has a good effect on the improvement of the conductive properties of asphalt concrete. Adding sufficient conductive phase material can make the resistivity of asphalt concrete meet the application requirements, but the volume parameter of concrete cannot meet [29]. However, the oil absorption of carbon black, the lubricity of graphite and the dispersibility of carbon fiber and steel fiber limit their content in asphalt concrete [30], respectively, resulting in the reduction of the stability of the electrical properties of conductive asphalt concrete. Moreover, for multi-conductive phase materials, the conductive mechanism is not clear. In addition, the influence of air void volume

Table 1
Research and application of Self-sensing asphalt concrete.

Author	Conductive filler used	Mixtures	Purpose
(Wu et al., 2005) [31]	Carbon black (CB), graphite (G), Carbon fibers (CF)	Stone mastic asphalt (SMA-13)	Electrical conductivity (Resistivity)
(Garcia et al., 2009)[32]	Steel wool, Graphite	Asphalt mortar/mastic (1.0-2.0 mm of crushed silica mineral)	Induction heating Electrical conductivity
(Liu et al., 2010, Quantao et al., 2012)[28,33]	Steel fibers, Steel wool	Porous asphalt concrete	Induction heating Electrical conductivity
(Liu X et al., 2009,2011) [30,34,35]	Graphite and carbon fiber	Asphalt concrete (Superpave12.5)	Piezoresistivity Mechanical property
(Menozzi et al.2015)[36]	Cast steel particles	Asphalt concrete	Self-healing
(Wang et al., 2016)[26]	Steel fibers, Graphite	Dense asphalt concrete (AC-13)	Electrical and mechanical properties Induction heating
(Liu et al., 2017) [37]	Steel fibers	Asphalt concrete (AC-16)	Induction heating
(Park, 2012, Rew et al., 2017) [38,39]	Graphite/ Carbon black	Asphalt mastic/ concrete (Superpave12.5)	Electrical and mechanical properties
(Xu et al., 2018, 2020)[24,40, 41]	Steel fibers, Calcium alginate capsules	Porous asphalt concrete	Combined healing system

(VV) on the electrical properties of conductive asphalt concrete needs further explanation.

The application of conductive technology in asphalt concrete has been proven to be feasible in technical demonstration and experimental exploration [42,43]. However, to realize the damage perception of asphalt pavement structure by using electrical signals, it is not necessary to have particularly excellent electrical properties (the existing conductive asphalt concrete is not suitable for self-sensing asphalt concrete), but only to ensure the stability of electrical signal conduction and the sensitivity of sensing signals in asphalt pavement structure. However, the existing research mainly focuses on induction heating, snow melting and self-healing, and the electrical diagnostic characteristics of asphalt concrete are slightly mentioned [44]. The existing conductive asphalt concrete only aims at maximizing its electrical performance based on road performance, thus ignoring the stability and sensitivity of its electrical performance. The research on the conductive mechanism of asphalt concrete mainly explores its electrothermal mechanism and pressure-sensitive characteristics, but does not deeply explore its electrical signal transmission mechanism, ignoring its transmission mechanism as an electrical signal to diagnose the structural damage of asphalt pavement[45]. In addition, the synergistic conductive mechanism of multiphase composite conductive materials and the self-sensing structural damage mechanism of conductive asphalt concrete are still unclear. These efforts collectively contribute to a more comprehensive understanding of the potential and limitations of conductive asphalt concrete.

Therefore, this study aims to design multi-phase composite modified self-sensing asphalt concrete by adding the conductive additives of graphite and steel fibers. Effects of volume parameters on the electrical properties of the self-sensing asphalt concrete are studied for electrical properties and stability. Influencing factors such as multi-conductive additives contents on the stability of electrical properties are clarified. The long-short synergistic conduction mechanism of multi-conductive asphalt concrete is revealed. The influence of different volume parameters on the electrical properties and stability of conductive asphalt

concrete is studied. Asphalt concrete crack propagation is directly related to the change of VV. The correlation analysis between VV and electrical properties of asphalt concrete is established. The flow chart of self-sensing asphalt concrete design is shown in Fig. 1.

2. Materials and experimental methods

2.1. Materials

2.1.1. Asphalt binders

Penetration grade 60/80 (i.e., Pen 60/80) was used as the asphalt binder. Technical properties of the asphalt binder are shown in Table 2.

2.1.2. Aggregates and fillers

The coarse aggregates (particle size > 2.36 mm) and fine aggregates (particle size of 0.075 – 2.36 mm) used are crushed limestones. The filler applied is the mineral powder grounded from the limestone. Technical properties of aggregates and fillers are shown in Tables 3 – 5.

2.1.3. Conductive additives

Asphalt concretes have been enhanced with the addition of graphite and steel fibers to serve as conductive additives for crack-sensing through electrical resistance. Fig. 2 illustrates the microscopic surface morphology of these additives, while Tables 6–7 presents their technical properties. Graphite, with its layered structure of graphene crystals, consists of carbon atomic layers arranged in a hexagonal lattice. The carbon atoms form covalent bonds with neighboring atoms, creating a planar lattice structure. The presence of unpaired electrons forms a free electron cloud, enabling the material to exhibit electrical conductivity when influenced by an external electric field. Steel fibers, ranging from 70 to 130 μm in diameter, offer the potential for improved charge transfer efficiency and speed due to their larger surface area and roughness. Additionally, the surface morphology of steel fibers impacts the contact area and quality with other conductive media, thereby influencing the overall conductivity performance.

Table 2
Technical properties of the Pen 60/80 asphalt binder.

Parameters	Units	Results	Requirements	Methods
Needle penetration (25 °C, 5 s, 100 g)	0.1 mm	74.0	60-80	ASTM D5
Softening point	°C	48.5	≥ 46	ASTM D36
Ductility (15 °C)	cm	> 100	≥ 100	ASTM D113
Density (15 °C)	g/cm ³	1.035	NA	JTG E20 T0603
Dynamic viscosity (60 °C)	Pa·s	261.0	≥ 180	JTG E20 T0620

Table 3
Technical properties of coarse aggregates.

Parameters	Units	Results	Requirements	Methods
Stone crushing value	%	21	≤ 28	JTG E42 T0316
Needle flake content	%	9.8	≤ 15	JTG E42 T0312
Los Angeles wear value	%	17	≤ 28	JTG E42 T0317
Water absorption	%	0.8	≤ 2.0	JTG E42 T0308
Apparent density	–	2.838	≥ 2.6	JTG E42 T0605

Table 4
Technical properties of fine aggregates.

Parameters	Units	Results	Requirements	Methods
Sediment percentage	%	2.7	≤ 3	JTG E42 T0335
Sand equivalent	%	78.3	≥ 60	JTG E42 T0334
Angularity (flow time method)	s	52.7	≥ 30	JTG E42 T0345
Apparent density	–	2.712	≥ 2.5	JTG E42 T0328

Table 5
Technical properties of the mineral powder.

Parameters	Units	Results	Requirements	Methods
Apparent density	–	2.701	≥ 2.50	JTG E42 T0352
Particle size range (%)				
< 0.6	mm	100	100	JTG E42 T0312
< 0.15	mm	97.3	90 – 100	JTG E42 T0317
< 0.075	mm	89.8	75 – 100	JTG E42 T0308
Plasticity coefficient	–	2.4	< 4	JTG E42 T0354
Hydrophilic coefficient	–	0.6	< 1	JTG E42 T0353

2.2. Development of self-sensing asphalt concrete

2.2.1. Mixture gradation

A dense-graded mixture was used, and the nominal maximum aggregate size was 13.2 mm (AC-13). The aggregates were divided into three grades: 10 – 15 mm, 5 – 10 mm and 0 – 5 mm. The composite aggregate gradation is shown in Fig. 3, and the mixing ratio of aggregates is shown in Table 8. The asphalt content was 4.9% by weight of aggregates [30,46]. Due to the addition of steel fibers and graphite as additives in asphalt mixtures, although the combined maximum volume fraction of steel fibers and graphite is less than 2%, the filling effect of the externally added conductive additives will slightly increase the content of fine aggregates in the mixture, thereby altering its gradation [46]. To minimize the impact of gradation, the synthetic gradation of fine aggregates (1.18–4.75 mm) approximates the lower limit of AC-13 grade.

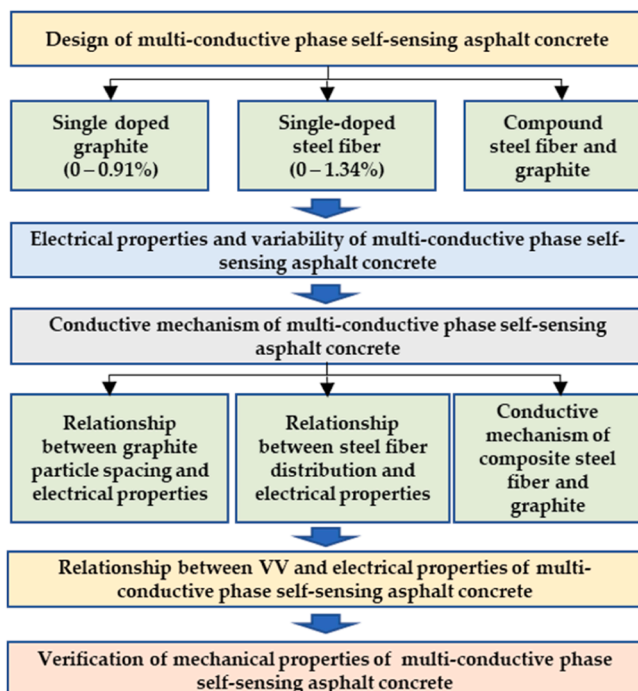


Fig. 1. Flow chart of self-sensing asphalt concrete design.

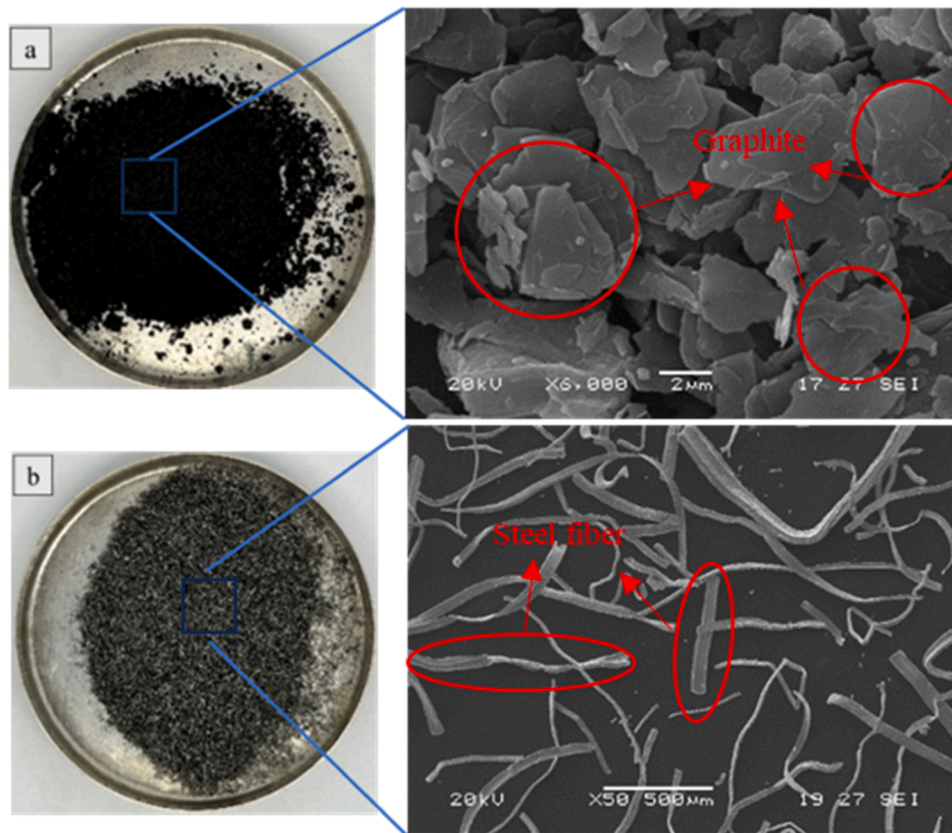


Fig. 2. Conductive additives (a. graphite; b. steel fiber).

Table 6
Technical properties of graphite.

Technical properties	Shape	Density (g/cm ³)	Specific surface area (m ² /g)	Particle size (mesh)	Carbon content (%)	Ash content (%)	Conductivity (Ω·m)
Results	Scaly shape	2.2	2.625	500	> 99	0.2	3.2 × 10 ⁻⁴

Table 7
Technical properties of steel fibers.

Technical properties	Shape	Density (g/cm ³)	Length (mm)	Diameter (μm)	Melting point (°C)	Conductivity (Ω·m)
Results	Fiber	7.8	4.2-4.8	70-130	1530	1.5 × 10 ⁻⁶

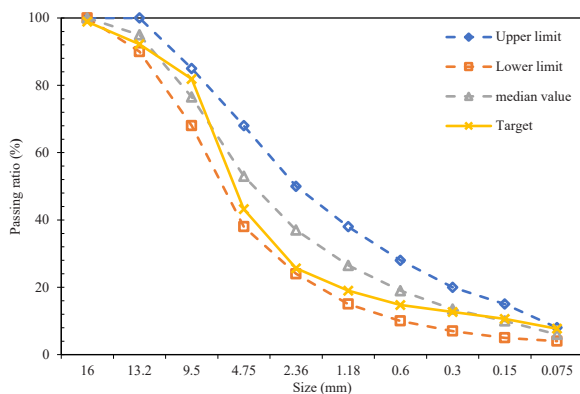


Fig. 3. Composite aggregate gradation.

Table 8
Mixing ratio of aggregates.

Aggregates	0-5	5-10	10-15	Filler
Mixing ratio (%)	42	35	10	3

2.2.2. Manufacturing process

The manufacturing process of self-sensing asphalt concretes is shown in Fig. 4. Steel fibers are added three times because they are prone to agglomerate. First, 1/3 of the steel fiber is added and mixed for 90 s when the aggregate is mixed. Next, another 1/3 of the steel fiber is added and mixed for 90 s when the asphalt is added. Then, the remaining steel fiber is added and mixed for 90 s when the mineral powder and graphite are added. Lastly, the Marshall design method was applied to double-sided compact the specimen for 75 times at 135 °C. The test specimens are shown in Table 9. Because the dosage of conductive materials in the existing research is not uniform [42,43], in

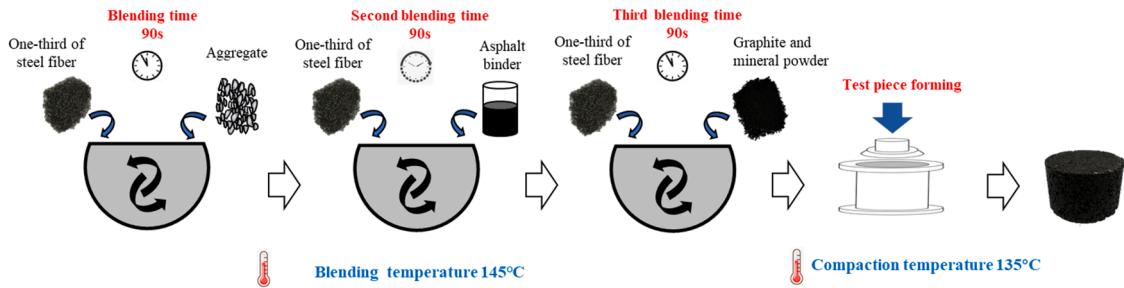


Fig. 4. The manufacturing process of self-sensing asphalt concretes.

Table 9
Test specimens.

Test specimens	Volume proportion of asphalt mixture (%)	
	Graphite	Steel fiber
Original-AC	—	—
Graphite-AC	0.05, 0.14, 0.23, 0.45, 0.68, 0.91	0
Steel fiber-AC	0	0.11, 0.23, 0.34, 0.46, 0.68, 0.80, 0.91, 1.02, 1.13, 1.34
0.9%Steel fiber + Graphite	0.23, 0.45, 0.68, 0.91	0.91
1.0%Steel fiber + Graphite	0.23, 0.45, 0.68, 0.91	1.02
1.1%Steel fiber + Graphite	0.23, 0.45, 0.68, 0.91	1.13

order to facilitate understanding, the dosage of conductive fillers in asphalt concrete is based on the proportion of asphalt concrete volume.

2.3. Experimental methods

2.3.1. Volume parameter test

The specimen is formed by Marshall Compaction, the molding temperature is 130 °C, the double-sided compaction is 75 times, and the specimen is demolded after 24 h. Each group contains four formed test pieces, and the volume parameters were tested. The volume parameter properties were characterized by the volume of air voids (VV), voids in mineral aggregate (VMA) and voids filled with asphalt (VFA). The formula for VV, VMA and VFA are shown in Eqs. (1)–(3), respectively.

$$VV = \left(1 - \frac{\gamma_f}{\gamma_t}\right) \times 100 \tag{1}$$

$$VMA = \left(1 - \frac{\gamma_f}{\gamma_{sb}} \times \frac{P_s}{100}\right) \times 100 \tag{2}$$

$$VFA = \frac{VMA - VV}{VMA} \times 100 \tag{3}$$

where, γ_f is the relative density of the gross volume of the specimen, γ_t is the theoretical maximum relative density of the asphalt concrete, P_s is the percentage of mineral aggregate in asphalt concrete (%), and γ_{sb} is the synthetic gross volume relative density of mineral aggregate.

2.3.2. Electrical resistance test

The electrical properties test was carried out at room temperature (25 °C), and the two sides of the up-down of the Marshall specimen were clamped with copper plate (the resistance of the copper plate was less than 1 Ω). Use an ohmmeter to directly measure the resistance of the upper and lower sides of the Marshall specimen. The ohmmeter model as well as the test procedure is represented in Fig. 5. Each group consists of 4 test pieces, and each test piece is measured 4 times, the ohmmeter range is shown in Table 10. According to the resistance data, the resistivity is obtained by the second Ohm’s law.

$$P = R \times \frac{S}{L} \tag{4}$$

where, P is the electrical resistance, measured in Ω·m; L is the internal electrode distance, measured in m; S is the electrode conductive area measured in m² and R is the measured resistance, measured in ohms (Ω).

To investigate the correlation between void fraction and electrical properties of conductive asphalt concrete, Marshall specimens were

Table 10
Ohmmeter range.

Technical indicator	Insulation ohmmeter	Ohmmeter
Range	4 MΩ-2200 MΩ	0-40 MΩ
resolution ratio	0.1 MΩ	0.001 MΩ
accuracy	±10%	±0.5%

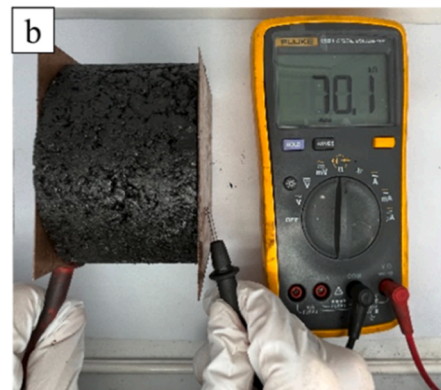
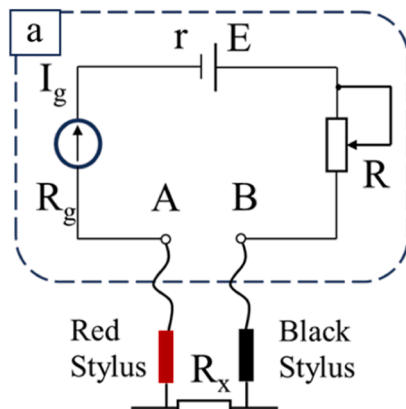


Fig. 5. Resistance meter model and test procedure (a: resistance meter model; b: test procedure).

prepared with varying compactions using double-side compaction for 40, 50, 60, 70, 75, 80, and 90 cycles, respectively, to achieve different void fractions. The void ratio of the Marshall specimens can be adjusted during preparation by subjecting them to varying work intensities, thus resulting in differing void ratios[47,48]. Four specimens in each group were utilized to measure their volume parameters and electrical properties. The porosity and electrical properties of conductive asphalt concrete exhibit a two-stage behavior, demonstrating a linear relationship when the void fraction meets the specified requirements. Conversely, when the void fraction exceeds the specified requirements, it shows an exponential relationship, as described in Eqs. (5) and (6).

$$\alpha = a \times \beta + b, 6 \geq \beta \geq 3 \tag{5}$$

$$\alpha = a \times e^{b\beta}, \beta \geq 6 \tag{6}$$

Among them, α is the volume resistivity of the test piece, β is the void fraction of asphalt concrete, and a and b are fitting parameters.

2.3.3. CT test

In this study, a GE Vtomex three-dimensional X-ray microscope was used to conduct three-dimensional CT (3D-CT) scanning of asphalt concrete with different contents of conductive additives to characterize its microscopic three-dimensional morphology and the conductive paths of conductive additives. During CT scanning, the test sample rotates synchronously with the rotary table. As the sample rotates at each small angle, a projection photograph can be obtained. CT tests were carried out on conductive asphalt concrete with steel fiber mass of 0.91%, 1.02%, 1.13% and 1.34%. Each sample size is 30 * 30 * 5 mm. Subsequently, 360° rotation and projection are carried out, the 3D reconstruction image is synthesized by VG studio, and the CT scanning image is processed by the reconstruction software Avizo.

2.3.4. Mechanical test

The mechanical properties of asphalt concrete were studied by the Marshall stability test and splitting test and adopted $\phi 101.6 \text{ mm} \times 63.5 \text{ mm}$ standard Marshall specimens. The Marshall stability test is to test the sample after 30 min of water bath at 60 °C, and the splitting test is to test the sample after 120 min of water bath at 25 °C. The loading rate is 50 mm/min.

3. Results and discussions

3.1. Volume parameters of self-sensing asphalt concrete

For the standard Marshall specimen of multiphase composite modified Self-sensing asphalt concrete, three volume parameters, namely VV, VMA and VFA, were measured respectively. The test results of VV, VMA, and VFA are shown in Fig. 6, Fig. 7, and Fig. 8. It can be seen from Fig. 6

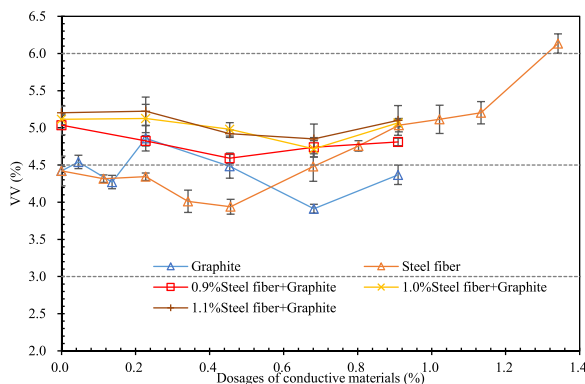


Fig. 6. Volume of air voids (VV) of asphalt concrete with different content of conductive additives.

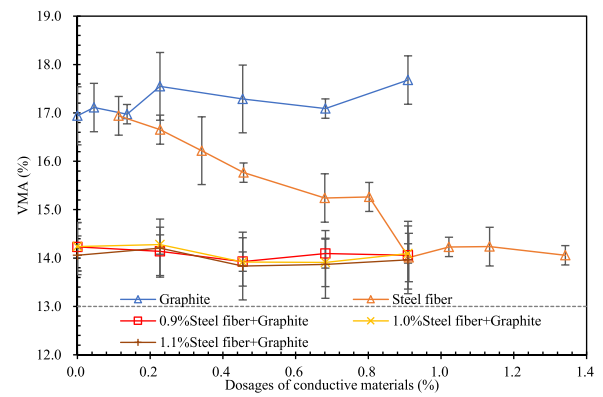


Fig. 7. Voids in mineral aggregate (VMA) of asphalt concrete with different content of conductive additives.

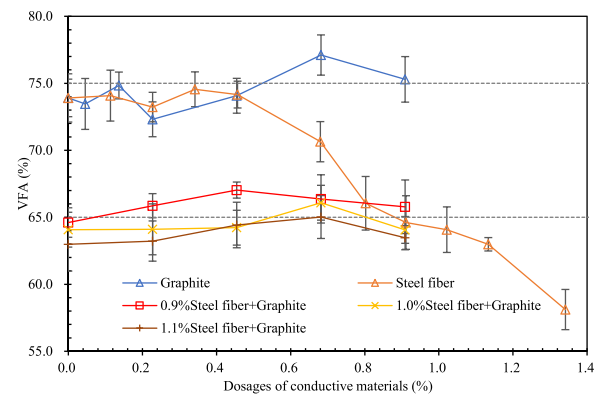


Fig. 8. Voids filled with asphalt (VFA) of asphalt concrete with different content of conductive additives.

that the small particle size of graphite, plays a role in filling and lubricating the mixture. When graphite is added alone, the VV of asphalt concrete with 0.23% graphite content is the largest, 4.86%, and the VV of asphalt concrete with 0.68% graphite content is the smallest, 3.91%. The change in graphite content has little impact on asphalt concrete, and the VV fluctuates around 4%, meeting the specification requirements; When steel fiber is added alone, VV decreases first and then increases with the increase of steel fiber content. The minimum VV of asphalt concrete with 0.46% steel fiber content is 3.94%, and the maximum VV of asphalt concrete with 1.3% steel fiber content is 6.13%. Moreover, when the steel fiber content is 1.3%, it does not meet the specification requirements; When graphite/steel fiber composite is modified, VV mainly increases with the increase of steel fiber, but all meet the requirements of 3 - 6% of the specification.

It can be seen from Fig. 7 that the VMA of asphalt concrete meets the requirements of the specification of more than 13%. With the increase of graphite content, the VMA tends to increase, while with the increase of steel fiber content, the VMA tends to decrease. It can be seen from Fig. 8 that when graphite is added alone, VFA tends to increase as a whole with the increase of graphite content, but when the graphite content reaches 0.68% or more, it does not meet the requirements of 65–75% of the specification; When steel fiber is added alone, VFA decreases with the increase of steel fiber content. When steel fiber reaches 0.9% or more, VFA is less than 65%, which does not meet the requirements of 65–75% of the specification; When graphite/steel fiber composite modification is used, the VFA of asphalt concrete mixed with graphite increases with the increase of graphite content, and decreases with the increase of steel fiber content. When the graphite content is less than 0.45% and the steel fiber content is more than 1.1%, the VFA of asphalt concrete mixed with asphalt does not meet the specification requirements. Graphite doping

will increase VFA, while steel fiber doping will reduce VFA. The increase caused by graphite is smaller than the decrease caused by steel fiber.

The density of graphite is less than that of aggregate and filler. With the increase in graphite content, the density of asphalt concrete decreases gradually. Moreover, the graphite particle size is only 500 meshes (0.025 mm), with a large specific surface area, more adsorbed asphalt, and lower content of free asphalt, which leads to the increase of effective asphalt mineral aggregate gap, VMA and VFA in asphalt concrete. Although the content of fine aggregate in the mixture increases and VV decreases slightly due to the addition of graphite, graphite absorbs more asphalt, which leads to the increase of the gap between mineral aggregate and the decrease of VV is not significant. The density of steel fiber is much higher than that of aggregate. With the increase of steel fiber content, the density of asphalt concrete increases gradually. The addition of steel fiber increases the content of fine aggregate in the mixture, but when the amount of steel fiber is too large, the mixture cannot be compacted, so VV decreases first and then increases, VMA and VFA decrease. For VFA, the increase caused by graphite is smaller than the decrease caused by steel fiber. Therefore, the graphite content of the composite graphite/steel fiber conductive asphalt concrete should not be less than 0.45% and the steel fiber content should not be more than 1.1% to meet the volume parameter requirements of asphalt concrete.

3.2. Electrical characteristics of self-sensing asphalt concrete

3.2.1. Effect of graphite content on electrical properties of asphalt concrete

The prepared original asphalt concrete and single graphite asphalt concrete specimens were tested for electrical properties. Due to the large resistance of single graphite asphalt concrete, a large range insulation ohmmeter is used. The electrical properties experimental results are shown in Fig. 9. It can be seen, that graphite conductive particles infiltrate and fill in asphalt mortar to form conductive particle chains to form conductive paths. However, the skeleton structure of aggregate in asphalt concrete leads to the increase of the spacing of conductive fillers in conductive paste, and the resistance of graphite asphalt concrete is high. The resistance of asphalt concrete decreases with the increase of graphite content. When the graphite content is less than 0.23%, the measured resistance is out of range and greater than 2.20×10^6 k Ω ; When the graphite content is 0.23%, the resistance of asphalt concrete is 1.79×10^6 k Ω , volume resistivity is 2.28×10^8 Ω -m. Therefore, when the graphite content is greater than 0.23%, the conductive graphite particles form a conductive carrier path and have conductivity.

The asphalt mortar part plays a conductive role in the conductive asphalt concrete. It forms a film on the surface of the aggregate, which connects the aggregate to form a continuous conductive path. The graphite conductive particles penetrate and fill in the asphalt mortar to form a conductive particle chain to form a conductive path. The change

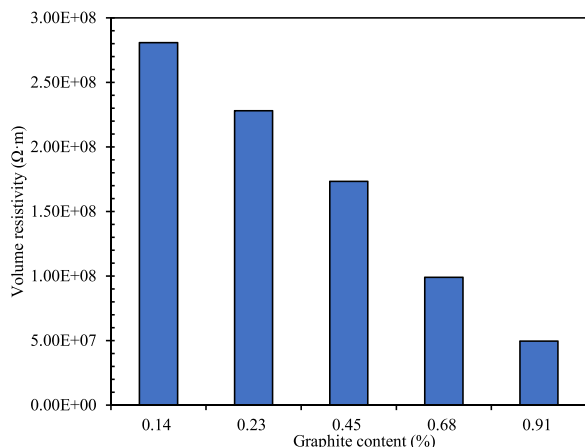


Fig. 9. Electrical resistance of asphalt concrete with different graphite content.

in the asphalt thickness of the graphite asphalt mortar can characterize the reason for the change in its conductivity to a certain extent. Asphalt film thickness calculation equation see (7) - (8):

$$SA = \sum (P_i \times FA_i) \tag{7}$$

$$DA = \frac{P_{be}}{\gamma_b \times SA} \times 10 \tag{8}$$

Among them, SA is the specific surface area of the filler, m^2/kg ; P_i is the percentage of filler mass, %; FA_i is the specific surface area coefficient of the corresponding fillers; DA is the effective thickness of asphalt film, μm ; P_{be} is the effective content of asphalt, %; γ_b is the relative density of asphalt ($25^\circ C/25^\circ C$).

Different graphite asphalt mortar film thickness calculation results are shown in Table 11. With the increase of graphite content, the thickness of asphalt film between graphite gradually decreases, and the spacing between graphite particles gradually decreases. The relationship between graphite particle spacing and resistivity is shown in Fig. 10. It can be seen from Fig. 10 that the graphite conductive particle spacing is logarithmically related to the resistivity of asphalt concrete, and the correlation coefficient is greater than 0.97. In composite materials doped with conductive additives, the conductive properties are generated from the conductive network formed by the overlapping of conductive particles. The conductive particles must reach a certain distance to conduct electricity. When the distance is greater than this distance, the conductivity between the conductive particles will fail. This distance is called the failure distance. When the volume fraction of graphite is more than 0.68%, the graphite spacing of asphalt mortar is less than $2 \mu m$, and the resistivity of conductive asphalt concrete is less than $10^8 \Omega \cdot m$, conductive properties are preliminarily obtained. Therefore, the failure distance of conductive particles doped with graphite alone is $2 \mu m$, and the volume content of graphite should not be less than 0.68% to have conductivity. When the tensile stress is applied to the material, the resistivity of the material increases due to the increase of the gap between the conductive particles; applied pressure is reversed, the resistivity of the material is reduced by shortening the gap between the conductive particles. The conductivity of conductive asphalt concrete is related to the spacing of its internal carriers. Its resistivity is inversely proportional to the spacing of carriers. Therefore, graphite conductive asphalt concrete has pressure sensitivity, which can be analyzed by the change of carrier spacing with load. In conclusion, the correlation between resistance and stress is related to the destruction and reorganization of conductive networks under stress.

3.2.2. Effect of steel fiber content on electrical properties of asphalt concrete

The prepared original asphalt concrete and single graphite asphalt concrete specimens were tested for electrical properties. When the steel fiber content is less than 0.46%, a large range ohmmeter is used for resistance measurement; When the content of steel fiber is more than 0.46%, a high-precision small range ohmmeter is used for resistance measurement. The resistance test results are shown in Fig. 11. The presence of steel fibers uniformly dispersed in the non-conductive

Table 11 Asphalt film thickness with different graphite content.

Calculation results	Volume fraction of graphite in asphalt (%)					
	0.6	1.5	2.4	4.6	6.9	9.3
Volume fraction of graphite in asphalt (%)	0.05	0.14	0.23	0.45	0.68	0.91
Asphalt mass fraction (%)	99	97	95	90	85	80
SA(m^2/kg)	26.25	78.75	131.25	262.5	393.75	525
Asphalt film thickness DA (μm)	36.40	11.89	6.99	3.31	2.08	1.47

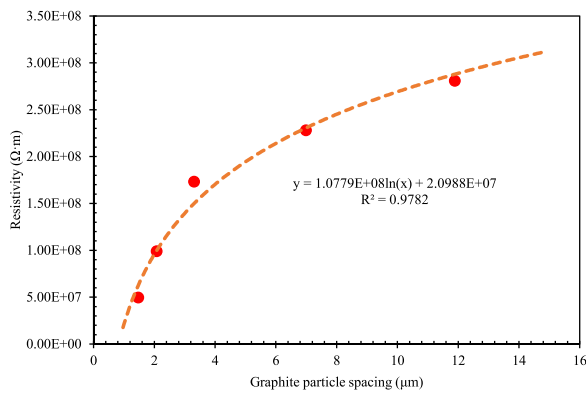


Fig. 10. Relationship between graphite particle spacing and resistivity of asphalt concrete.

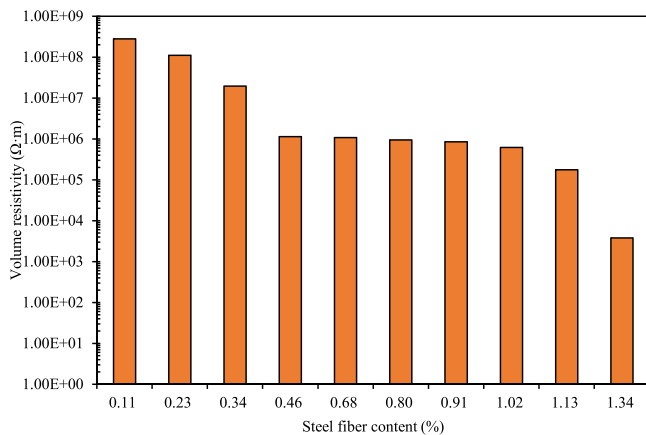


Fig. 11. Conductivity of asphalt concrete with different steel fiber content.

asphalt concrete facilitates electrical conductivity by establishing a coherent network structure, enabling effective communication between the fibers. It can be seen from Fig. 11 that the resistance of asphalt concrete decreases with the increase of steel fiber content. With the change of steel fiber content, the resistance of asphalt concrete presents four stages: (1) 0 – 0.46% steel fiber, failed to form a tunneling conductive network, asphalt concrete is the insulating phase, and the steel fiber is completely separated, no conductive path and the resistivity greater than $10^7 \Omega\cdot\text{m}$; (2) 0.46–0.80% steel fiber, The asphalt concrete forms a tunneling conductive network, and the fibers are evenly dispersed in the matrix, which is semi-conductive, the steel fiber in the concrete forms a partial path and resistivity is $10^6\text{--}10^7 \Omega\cdot\text{m}$; (3) 0.80–1.13% steel fiber, The conductive fibers are partially agglomerated under dispersion conditions. With the increase of steel fiber content, the resistance decreases more slowly, and resistivity is $10^6 \Omega\cdot\text{m}$; (4) The content of steel fiber is more than 1.13%, Stacking or entanglement between steel fiber. Asphalt concrete is conductive phase, asphalt concrete and steel fiber overlap each other to form a path. The resistance is relatively small, and the resistivity is less than $10^6 \Omega\cdot\text{m}$.

The microstructure of conductive asphalt concrete was studied by the 3D-CT scanning method. In this study, CT tests were carried out on conductive asphalt concrete with steel fiber mass of 0.9%, 1.0%, 1.1% and 1.3%. Each sample size is $30 \times 30 \times 5 \text{ mm}$. The two-dimensional projection of CT in the middle of the four groups of specimens is shown in Fig. 12, and the three-dimensional reconstruction is shown in Fig. 13. It can be seen from the two-dimensional image that with the increase of steel fiber content, the conductive path of conductive asphalt concrete gradually increases, and its resistivity gradually decreases. It can be seen from Fig. 12-c and Fig. 12-d that as the steel fiber content

increases from 1.1% to 1.3%, the conductive path does not increase significantly, the asphalt mortar part increases, the VV increases, the mechanical properties decrease, and the electrical properties decrease slowly. The results of the CT image are consistent with the test results of mechanical and electrical properties.

From the three-dimensional distribution of conductive asphalt concrete in Fig. 13, the distribution of conductive phase materials in asphalt concrete is relatively uniform. Conductive asphalt concrete is mainly composed of two parts, one part is aggregate accounting for about 90% of the weight, it is mainly composed of various specifications of aggregate to form a certain gradation, forming the skeleton structure of concrete, and this part is not conductive, another part is the asphalt mortar composed of mineral powder, asphalt and conductive phase materials [49]. This part of the asphalt mortar plays a conductive role, which forms a layer of film and grid on the surface of the aggregate and connects the aggregate to form a continuous conductive path. The conductivity of a substance depends on its microstructure [30]. Fig. 13 illustrates the three-dimensional structure of conductive asphalt concrete infused with graphite and steel fiber, showing the distribution of conductive phase materials within the asphalt concrete. The addition of steel fibers and their increased content facilitates the formation of a continuous conductive path in the asphalt concrete, thereby transforming the material from a highly insulating state to a conductive one. By the findings shown in Fig. 13, it is apparent that an increase in steel fiber content from 0.9% to 1.1% results in a distinct improvement in the conductive path, consequently leading to a gradual reduction in resistivity. However, upon further escalation of the steel fiber content from 1.1% to 1.3%, no significant enhancement in the conductive path is observed. This transition period coincides with an augmentation in the volume fraction of asphalt mortar, corresponding to an increase in mechanical properties but a gradual decline in electrical properties.

3.2.3. Coupling effect of graphite and steel fiber on electrical properties of asphalt concrete

Multi-phase composite modified self-sensing asphalt concrete specimens were tested for electrical properties. The resistivity of asphalt concrete with different content of conductive additives is shown in Fig. 14. The conductivity of conductive asphalt concrete is formed by the conductive network frame formed by the uniform distribution of steel fiber in the non-conductive asphalt concrete and the conductive particle chain formed by the penetration of graphite conductive particles into the asphalt concrete. It is manifested in the synergistic effect of fiber bridging and particle penetration, which is mainly conducted by the conductive network composed of steel fibers to form a conductive path inside the non-conductive asphalt concrete [38,39]. Therefore, the resistance of asphalt concrete decreases with the increase of the content of conductive additives. Adding graphite based on steel fiber can effectively improve the electrical properties of asphalt concrete. Compared with the single addition of 0.9%, 1.0% and 1.1% steel fiber asphalt concrete, the resistance of the composite addition of 0.91% graphite asphalt concrete decreased by 76.07%, 90.26% and 97.13% respectively. Due to the bridging effect of steel fiber, the low content of steel fiber does not form a path, and the electrical properties of asphalt concrete is generally improved by adding graphite based on 0.9% or less of steel fiber; When the content of steel fiber reaches 0.9%, the electrical properties of asphalt concrete can be improved by adding graphite; When the steel fiber content is more than 1.1%, the electrical properties of asphalt concrete increases slightly, and the steel fiber reaches saturation.

From the electrical properties and volume parameters of conductive asphalt concrete, asphalt concrete has better volume parameters, but the resistivity is too large and the electrical properties are poor. When steel fiber is added alone, the content of steel fiber is not less than 0.9%. Asphalt concrete has excellent electrical properties, but its volume parameters do not meet the requirements of the specification. In the mixed graphite/steel fiber conductive asphalt concrete, to meet the

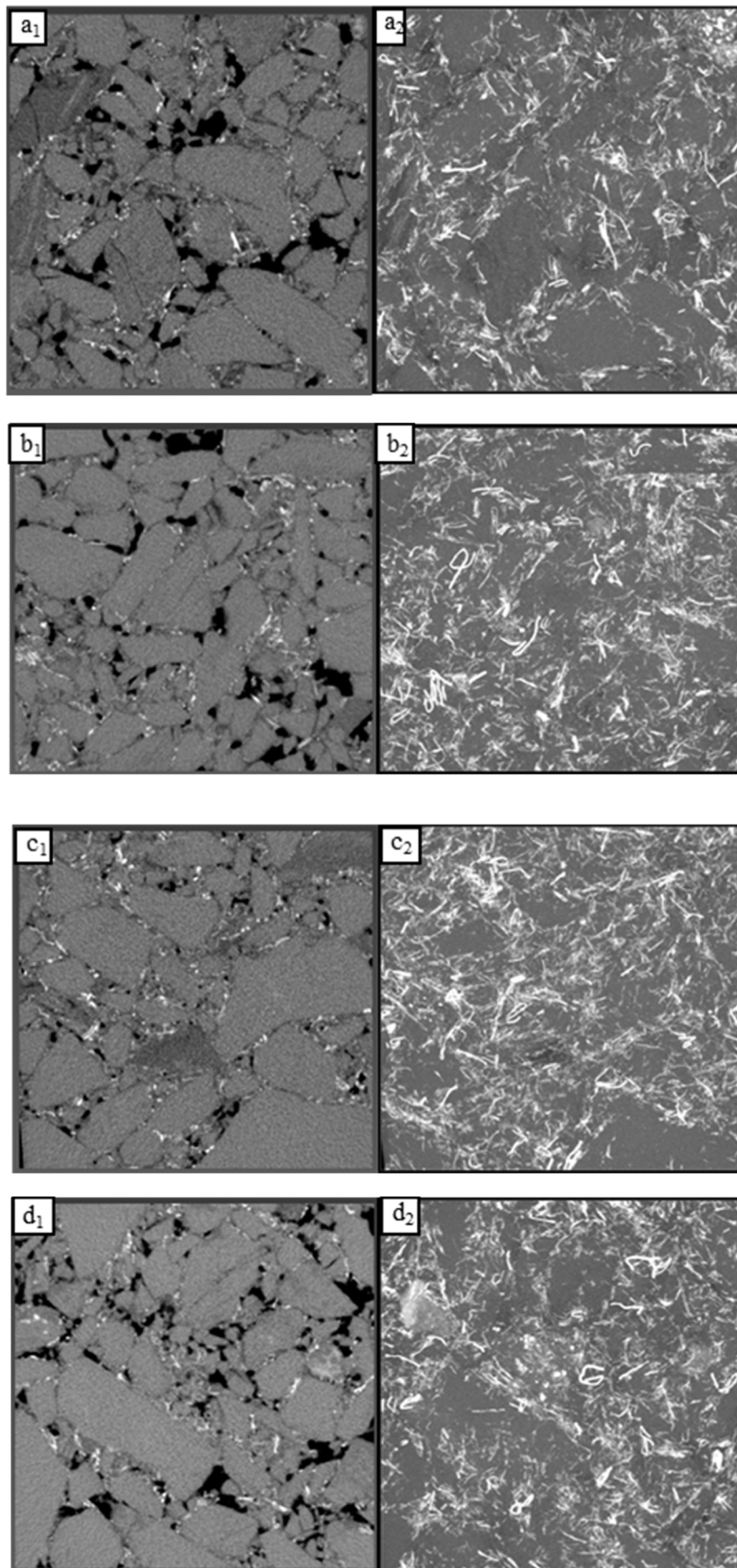


Fig. 12. CT two-dimensional projection and steel fiber distribution in conductive asphalt concrete (2D projection image specimen are 30 *30 mm.; a: 0.9% steel fiber + 0.68% graphite; b: 1.0% steel fiber + 0.68% graphite; c: 1.1% steel fiber + 0.68% graphite; d: 1.3% steel fiber + 0.68% graphite; a₁-d₁: two-dimensional projection; a₂-d₂: steel fiber distribution).

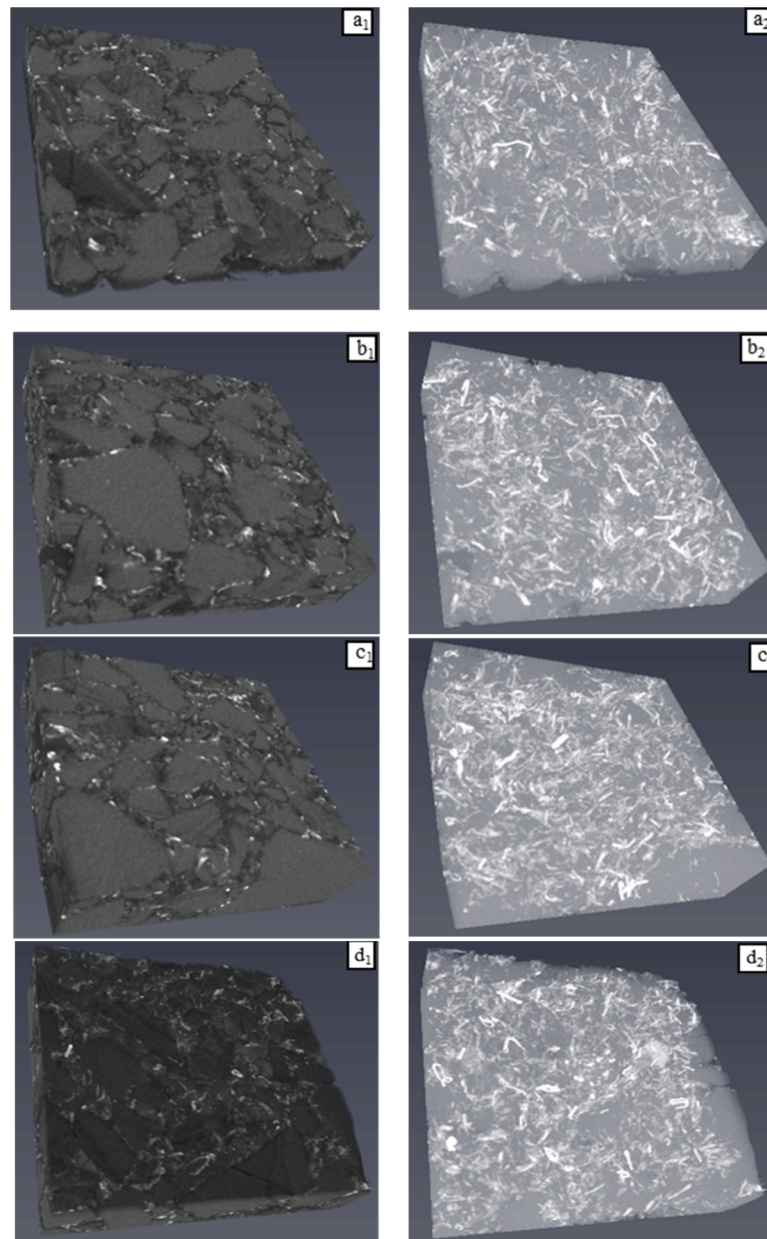


Fig. 13. Three-dimensional structure of conductive asphalt concrete (a: 0.9% steel fiber + 0.68% graphite; b: 1.0% steel fiber + 0.68% graphite; c: 1.1% steel fiber + 0.68% graphite; d: 1.3% steel fiber + 0.68% graphite; a₁-d₁: three-dimensional structure; a₂-d₂: steel fiber distribution).

requirements of asphalt concrete volume parameters. the graphite content should not be less than 0.45%, and the steel fiber content should not be more than 1.1%, to establish the correlation between the electrical properties and failure state of asphalt concrete under the premise of suitable resistance range, small resistance variability area and asphalt concrete volume parameters meeting the requirements, it is necessary to compound the conductive phase materials of self-sensing asphalt concrete. Therefore, the properties of asphalt concrete with 0.9%, 1.0% and 1.1% steel fiber and different content of graphite were studied.

3.3. Variability assessment of electrical characteristics of self-sensing asphalt concrete

The achievement of structural self-sensing in asphalt pavement relies on incorporating conductive asphalt concrete and upholding the steadfastness of its electrical characteristics. The variability of electrical properties characteristics of self-sensing asphalt concrete is assessed in

this section. Conductive asphalt concrete resistivity standard deviation is shown in Fig. 15, single mixed with conductive additive and multi-phase conductive additives of asphalt concrete electrical properties coefficient of variation are shown in Fig. 16 and Fig. 17, respectively. It can be seen from Fig. 15 that with the increase of conductive phase materials, the electrical conductivity of conductive asphalt concrete becomes better, the standard deviation of resistivity decreases gradually, and the fluctuation range of resistivity decreases gradually. From Fig. 16, graphite single dosage is not more than 0.68%, the resistivity of asphalt concrete coefficient of variation around 0.12; When the content of graphite is 0.91%, due to the excessive content of graphite in asphalt concrete, it is not easy to fully mix and the resistivity variation coefficient increases by 0.05. When the content of steel fiber is less than 1.0%, with the increase of steel fiber content, the electrical conductivity of asphalt concrete becomes better, and the coefficient of variation of resistivity decreases gradually. When the steel fiber content is greater than 1.0%, with the steel fiber content is too much, although the resistivity of

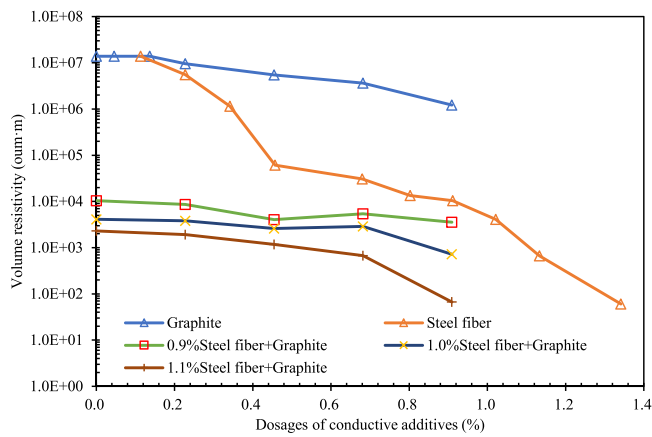


Fig. 14. Resistivity of asphalt concrete (upper and lower) with different amounts of conductive additives.

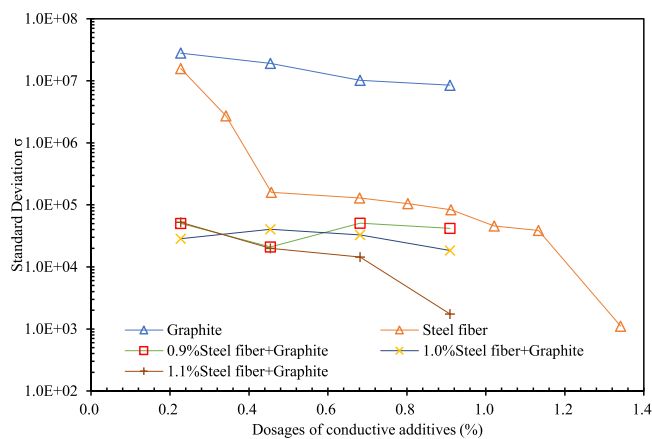


Fig. 15. Standard deviation of resistivity of conductive asphalt concrete.

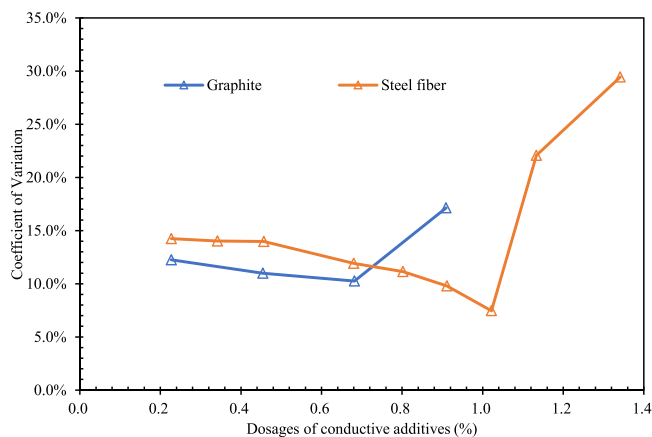


Fig. 16. Variation coefficient of electrical properties of asphalt concrete mixed with single conductive additive.

asphalt concrete decreases, it is difficult to dense asphalt concrete, VV is larger, the resistivity fluctuation becomes larger, leading to the increase of the resistivity coefficient of variation of asphalt concrete. It can be seen from Fig. 17 that the test group with small resistivity of asphalt concrete mixed with conductive additive has a large coefficient of variation. Due to the gradual increase of conductive phase additive, conductive additive gradually excess, although the resistivity is reduced, but the variation of resistivity fluctuation increases, the coefficient of

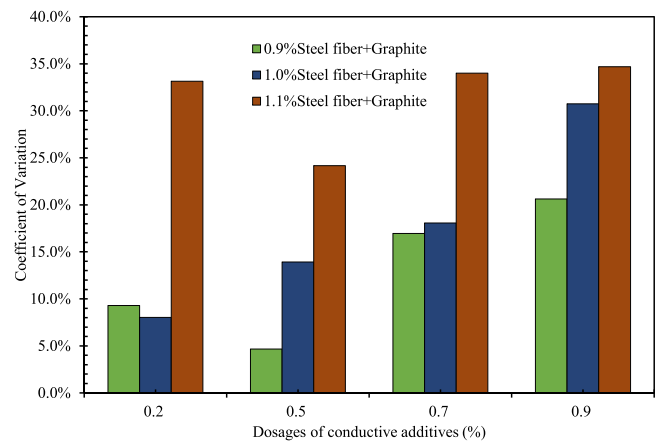


Fig. 17. Variation coefficient of electrical properties of asphalt concrete mixed with composite conductive additives.

variation increases. Considering the variability of electrical properties, when the content of steel fiber is less than 1.1% and the content of graphite is less than 0.91%, the resistivity variability of conductive asphalt concrete is small, and the coefficient of variation is less than 0.2.

3.4. Conductivity mechanism of self-sensing asphalt concrete

The research on the conductive mechanism of self-sensing asphalt concrete is of great significance for establishing self-sensing of intelligent pavement. Moreover, the perfect conductive mechanism is necessary to deeply understand the performance of self-sensing asphalt concrete and further optimize the design of self-sensing asphalt concrete with better performance. In conductive asphalt concrete, the conductive behavior of conductive additives after forming a conductive path mainly involves the interface between conductive fillers, including the conductive path theory, tunnel effect theory and electric field emission theory [50]. According to the theory of conductive pathway [51], conductive particles are connected to form a chain of electrons, which generates conductive phenomena through chain movement. It is generally believed that conductive paths can be formed if conductive particles can contact each other or the gap between particles is small to form electron penetration. Therefore, the contact resistance and particle spacing of conductive particles are important factors affecting the conductivity. According to the theory of tunneling effect [52], in addition to the mutual contact between particles, electrons can also migrate in the gap of conductive particles dispersed in the matrix to produce conductive phenomena. According to the electric field emission theory, the emission current is generated due to the high electric field between conductive particles, such as the problem of non ohmic voltage current characteristics of composite materials. Study on conductive asphalt concrete, with the increase of the volume proportion of conductive additives, the conductivity of asphalt concrete has four stages [32]: (1) insulation stage, due to the low content of conductive additives, conductive fibers and fillers are separated, making the resistivity of asphalt concrete approximately similar to that of ordinary asphalt concrete; (2) transition stage, the first conductive path is formed and the asphalt concrete conducts electricity initially; (3) conductive stage, the electrical conductivity of asphalt concrete is good, and the conductive additives in asphalt concrete are dispersed to the largest extent. This node is the best content of conductive additives in conductive asphalt concrete; (4) excess conductive additives, the conductive asphalt concrete reaches the shortest conductive path, and the conductivity will not increase with the increase of the volume of conductive particles.

In general, the conductive phenomenon of conductive composites is caused by the comprehensive process of direct contact of conductive fillers and tunneling effect between gaps. However, there is a conductive

threshold between the volume proportion of conductive additives and the conductivity of asphalt concrete [53]. Adding conductive filler is helpful to short-circuit the ionic conductance path, so that asphalt concrete has stable resistivity. The resistivity of concrete will change with the content of conductive additives, that is, seepage and tunneling, as shown in Fig. 18: (1) When the content of conductive or semiconductor filler is low, the resistance of conductive asphalt concrete will not change much, and the resistance of conductive asphalt concrete is dominated by long-distance electron tunneling; (2) When the conductive filler reaches a certain value (percolation threshold), the resistance of conductive asphalt concrete will change significantly, that is seepage occurs, and the resistance of composite materials is dominated by tunnel conduction and contact conduction; (3) When the content of conductive or semiconductor filler continues to increase to a certain value, the conductive fillers partially aggregate, and the resistance of the composite tends to be stable, and the resistance of the composite is mainly contact conduction. Self-sensing concrete needs to have low resistivity, that is, stable resistance, and high sensing sensitivity, that is, high resistivity change rate, so the content range of self-sensing concrete filler is suggested to be near the percolation threshold.

As can be seen from Fig. 14 and Fig. 17, when the resistivity is high, the acquisition of electrical parameters cannot be realized. When the resistivity is low, the amount of conductive filler is often high, which makes it easy to agglomerate and form disorderly uneven dispersion in asphalt concrete, and the resistivity stability is poor. From Fig. 19, it can be seen that the combined use of fillers with different scales will produce a composite effect that a single filler does not have, and it can produce synergistic or multi-scale effects, that is, long-short distance synergistic conduction [26]. Steel fiber and graphite modified asphalt concrete carrier is mainly electrons [38,39]. There are three paths of current conduction in conductive asphalt concrete [50]: (a) Electrons are conducted through a conductive network composed of steel fibers; (b) Electrons are conducted through channels formed by overlapping steel fibers with graphite; and (c) Electrons are conducted through channels formed by graphite in contact with each other. Since the steel fiber and graphite are randomly distributed in the asphalt concrete, generally the above three conduction paths exist at the same time, one or two mechanisms mainly depend on the amount of fiber and graphite in asphalt concrete. When the content of steel fiber is more than 1.1%, the conductive mechanism is mainly conducted by the conductive network composed of steel fiber, the path formed by steel fiber and graphite and the penetration of graphite particles play an auxiliary role. When the content of steel fiber is 0.9–1.1%, the steel fiber does not completely form channels, and the fiber spacing is small, so the conductivity is dominated by the penetration spacing between graphite particles. The trend of properties test results is consistent with the change in 3D image.

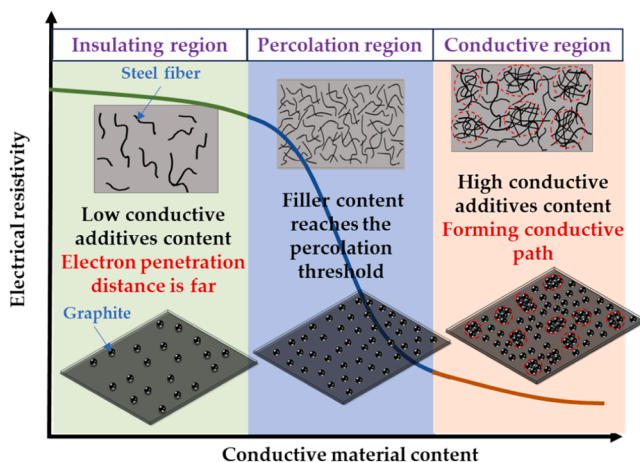


Fig. 18. Conductive mechanism of self-sensing asphalt concrete.

The conductive path formed by steel fiber has little variability in electrical properties. Damage to the internal structure of self-sensing asphalt concrete will lead to an increase in the spacing of conductive particles such as graphite, and a decrease in electron penetration and tunneling, which is reflected in the deterioration of its electrical properties.

3.5. Electrical sensitivity of self-sensing asphalt concrete to air void volume

Before the pavement structure is destroyed, the internal cracks gradually increase, showing loose particles and larger voids, which is similar to the process of air void volume (VV) increase. The electrical properties of the conductive asphalt concrete are negatively correlated with the VV of concrete. The change of resistivity of asphalt concrete can be used to predict the damage state inside the pavement structure. The smaller the VV of conductive asphalt concrete, the more stable the electrical properties and the smaller the variability. Therefore, in engineering applications, it is necessary to reduce the VV of conductive asphalt concrete as much as possible to ensure the stability of its electrical properties, and then improve the accuracy of its structural self-sensing.

Considering the volume parameters, electrical properties and mechanical properties of asphalt concrete, 0.9–1.1% steel fiber + 0.68% graphite conductive asphalt concrete has excellent properties. The proportion of conductive asphalt concrete with 0.9%, 1.0%, 1.1% steel fiber + 0.68% graphite was selected to prepare Marshall specimens with different compaction times. The Marshall specimens are shown in Fig. 20, and the porosity test results are shown in Fig. 21. It can be seen from Fig. 20 and Fig. 21 that with the increase of the number of compactions, the surface of Marshall gradually compacts and VV gradually decreases and stabilized. When the number of times of compaction 40–60, VV shows a gradual decrease, with the increase of the number of times of compaction, the mutual repulsive force between the particles gradually reduces, the gap between the particles is filled, the particles are more densely arranged, the asphalt will also better penetrate into the mixture in the voids, filling and bonding of the particles, so that the voids inside the mixture are reduced. When the number of times of compaction 60–80, due to the increase in the amount of steel fiber content, resulting in the work of the compaction strength is not sufficient to allow the VV to get a significant reduction. When the number of compaction times increased from 40 to 60 times, the VV of the three proportions of the mixture decreased significantly, and the VV of 0.9%, 1.0% and 1.1% Steel fiber+ 0.68% Graphite decreased by 39.57%, 49.58% and 54.06%, respectively. When the number of compaction times increased from 60 times to 80 times, the VV of 0.9% Steel fiber+ 0.68% Graphite decreased by 22.05%, due to the increase of steel fiber content in conductive asphalt concrete, the void of asphalt concrete was large, the specimen was difficult to compact, and the VV decrease was small, and the VV of 1.0% and 1.1% Steel fiber+ 0.68% Graphite decreased by 2.22% and – 7.34%, respectively. When the number of compactions reaches more than 80 times, due to the large compaction work, the limestone aggregate part of the asphalt concrete is crushed, the fine aggregate increases, and the asphalt concrete is significantly more compact, compared with 80 compactions, the VV of the three mixtures with 90 times is reduced by 21.83%, 25.23% and 22.89%, respectively. When the number of compactions increases from 60 to 80 times, the VV of 0.9% Steel fiber + 0.68% Graphite decreases by 22.05%. Due to the increase of steel fiber content in conductive asphalt concrete, the porosity of asphalt concrete is too large, the specimen is difficult to compact, and the VV decreases slightly. The VV of 1.0% and 1.1% Steel fiber + 0.68% Graphite decreases by 2.22% and – 7.34%, respectively. When the number of compactions reached more than 80 times, due to the larger compaction work, the limestone aggregate in the asphalt concrete was crushed, the fine aggregate increased, and the asphalt concrete was significantly denser. Compared with 80 times of compaction, the VV of the three mixtures was reduced by 21.83%,

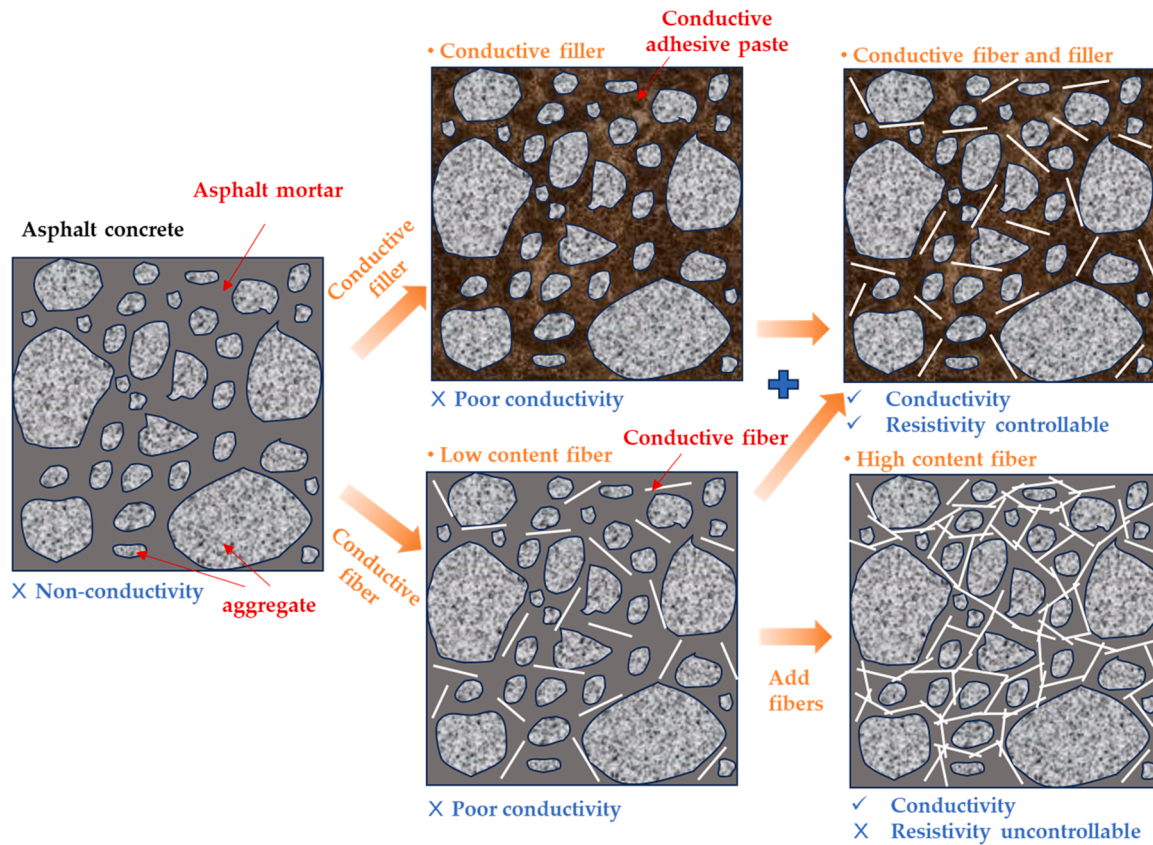


Fig. 19. Conductive mechanism of asphalt concrete modified by multi-conductive phase materials.

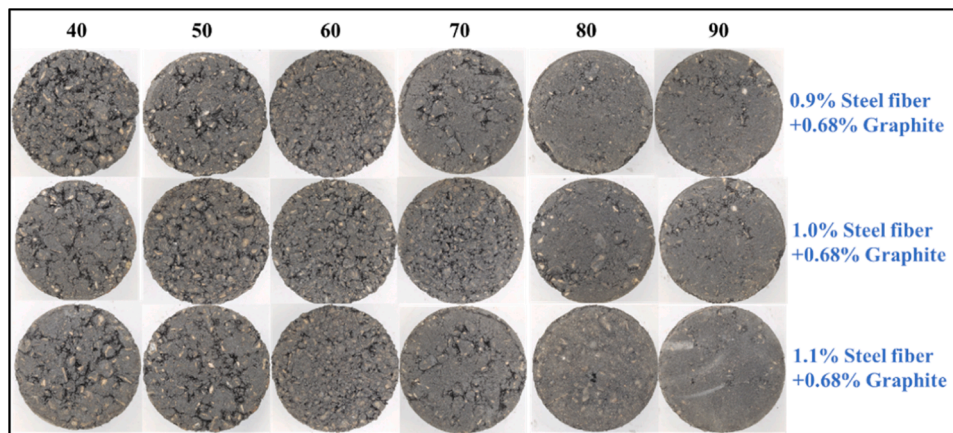


Fig. 20. Marshall specimens with different compaction times.

25.23% and 22.89% respectively after 90 times of compaction.

The relationship between VV and electrical properties of three proportions of conductive asphalt concrete are shown in Fig. 22, Fig. 23 and Fig. 24. The relationship between resistivity and VV is shown in Table 12. It can be seen from Fig. 22, Fig. 23 and Fig. 24 that when VV is 3–6%, the VV of concrete meets the requirements of the specification, and the VV of conductive asphalt concrete with three proportions is linearly related to the electrical properties, with the correlation coefficient R^2 being greater than 0.8; When VV is greater than 6%, the VV of the three proportions of conductive asphalt concrete is exponentially related to the electrical properties, and the correlation coefficient R^2 is all greater than 0.9, so the correlation degree is high. With the increase of VV, the resistivity increases rapidly. Because the conductive

mechanism of conductive asphalt concrete is mainly conducted by a conductive network composed of steel fibers. With the increase of conductive phase materials, the conductive paths of asphalt concrete gradually increase, and the conductive additives are surplus. The influence of VV gradually decreases. The higher the content of conductive additives, the lower the correlation. The larger the VV, the greater the resistivity of conductive asphalt concrete and the higher the variability.

For the service process of asphalt concrete pavement, the internal structure of asphalt concrete has experienced the following three stages [50]: in the early stage of fatigue loading, the porosity decreases, the contact between aggregates becomes closer, the spacing between conductive particles decreases, and the resistivity decreases. Then as the loading continues, the damage begins to appear, the internal porosity of

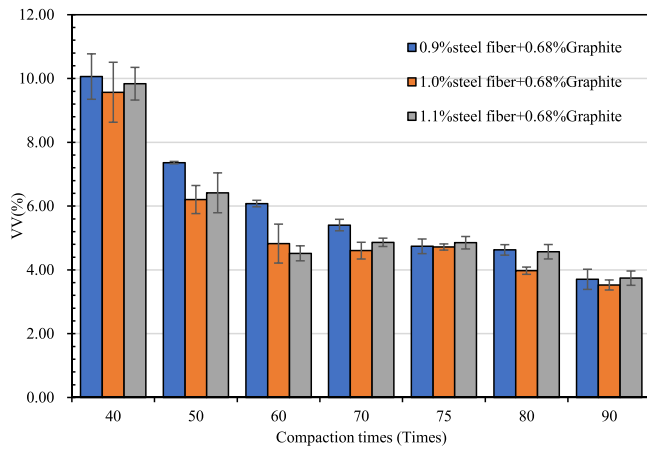


Fig. 21. Asphalt concrete volume of air voids (VV) with different compaction times.

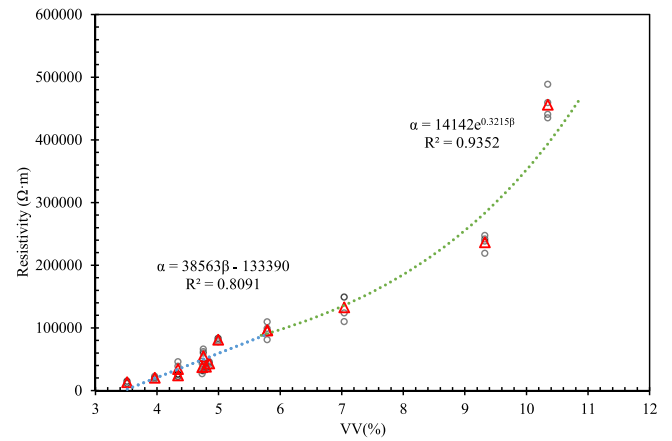


Fig. 24. Electrical properties of 1.1% steel fiber + 0.68% graphite conductive asphalt concrete of different volume of air voids (VV).

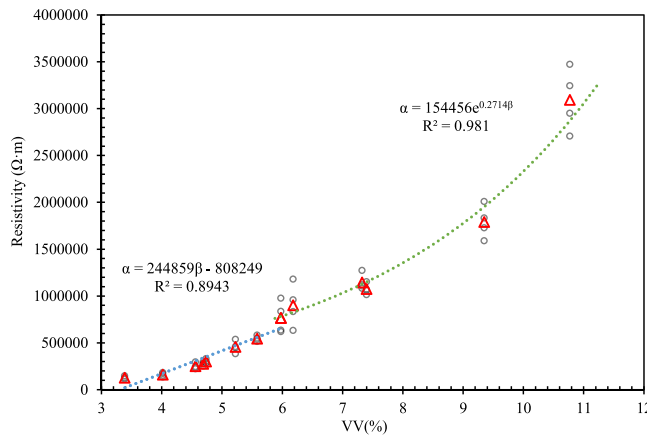


Fig. 22. Electrical properties of 0.9% steel fiber + 0.68% graphite conductive asphalt concrete of different volume of air voids (VV).

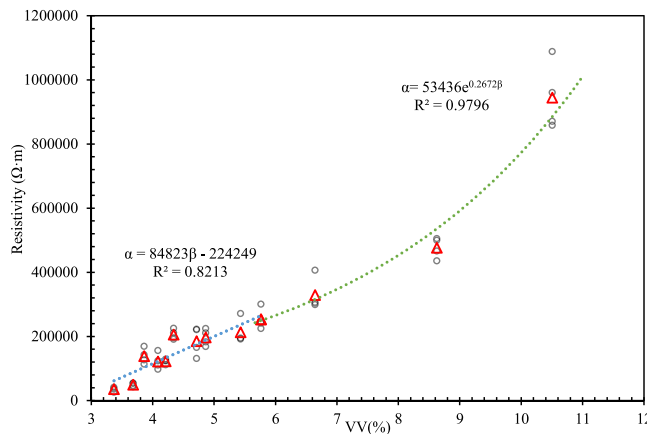


Fig. 23. Electrical properties of 1.0% steel fiber + 0.68% graphite conductive asphalt concrete of different volume of air voids (VV).

the mixture gradually increases, and the resistivity begins to increase slightly. In the later stage of loading, the micro-damage gradually developed and expanded, large cracks appeared, and the porosity of the mixture increased sharply, destroying the specimen, and then the conductive path was disconnected, and the resistivity increased greatly, even without conductivity. As shown in Table 12, VV of 3–6% belongs to

Table 12

Relationship between VV and resistivity (in the table, α is the resistivity of asphalt concrete; β is the VV of asphalt concrete).

Type of mixture	The VV range is 3 - 6%		VV is higher than 6%	
	Equation of VV and resistivity ($\Omega\cdot m$)	R^2	Equation of VV and resistivity ($\Omega\cdot m$)	R^2
0.9% steel fiber+ 0.68% graphite	$\alpha = 244859\beta - 808249$	0.8943	$\alpha = 154456e^{0.2714\beta}$	0.9810
1.0% steel fiber+ 0.68% graphite	$\alpha = 84823\beta - 224249$	0.8213	$\alpha = 53436e^{0.2672\beta}$	0.9796
1.1% steel fiber+ 0.68% graphite	$\alpha = 38563\beta - 133390$	0.8091	$\alpha = 14142e^{0.3215\beta}$	0.9352

the initial and medium-term changes of asphalt concrete fatigue loading; When VV is greater than 6%, the resistivity increases greatly with the increase of VV, which belongs to the late loading period of asphalt concrete, and the micro-damage develops and expands slowly. The change in concrete resistivity in fatigue process is mainly caused by the change in porosity. On the contrary, by studying the change of resistivity, we can also understand the change of internal structure of concrete and realize the self-sensing effect of internal structure of asphalt concrete.

3.6. Mechanical property evaluation of self-sensing asphalt concrete

Self-sensing asphalt concrete should not only ensure the stability of electrical properties, but also cannot ignore the changes of its mechanical properties. The influence of conductive additives on the mechanical properties of asphalt concrete is assessed in this section. The Marshall stability and splitting strength tests were carried out on the standard Marshall specimens of multiphase composite modified self-sensing asphalt concrete with different amounts of conductive additives, and the results of Marshall stability and splitting strength tests were shown in Fig. 25 and Fig. 26, respectively. It can be seen from Fig. 25 and Fig. 26 that the Marshall stability and splitting strength of asphalt concrete increase with the increase of graphite content due to the filling effect of graphite on the mixture. The Marshall stability and splitting strength of the original asphalt concrete were 8.43 kN and 0.83 MPa, respectively, which met the specifications. Compared with the original asphalt concrete, the Marshall stability of graphite asphalt concrete with single doped 0.23%, 0.45%, 0.68% and 0.91% increased by 18.03%, 27.76%, 35.71% and 39.62%, and the splitting strength increased by

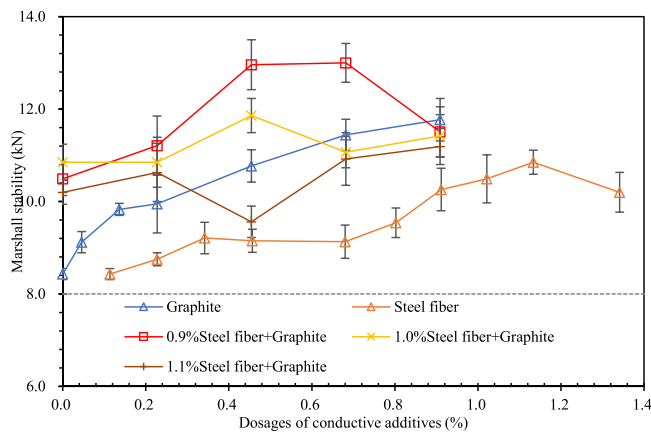


Fig. 25. Marshall stability of asphalt concrete with different amounts of conductive additives.

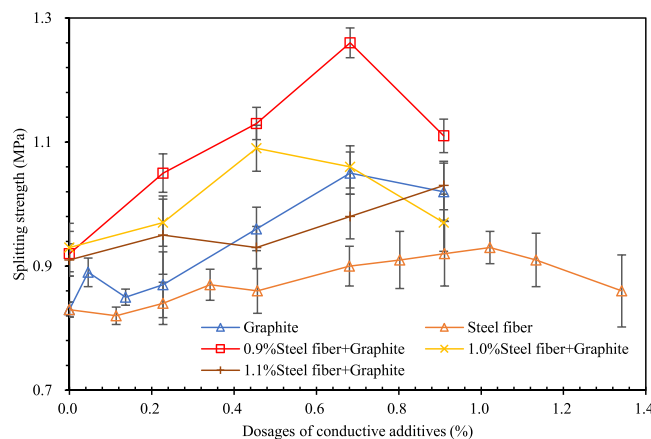


Fig. 26. Split strength of asphalt concrete with different amounts of conductive additives.

4.82%, 15.66%, 26.51% and 22.89%, respectively. It shows that the addition of graphite can better improve the mechanical properties of asphalt concrete. For single-doped steel fibers, the Marshall stability and splitting strength of asphalt concrete first increase and then decrease with the increase of steel fiber content. Steel fibers can form a network skeleton structure in the mixture to increase its mechanical properties but too many steel fibers will cause the asphalt concrete to be difficult to compaction, but lead to low compaction and reduced mechanical properties. When the steel fiber content is 1.0%, the Marshall stability and splitting strength of asphalt concrete are the largest, which are 10.85 kN and 0.93 MPa. Compared with the original asphalt concrete, the Marshall stability of 2.5%, 0.9%, 1.0%, 1.1% and 1.3% steel fiber asphalt concrete increased by 21.71%, 24.44%, 28.71%, 21.00% and 14.71%, and the splitting strength increased by 9.64%, 10.84%, 12.05%, 9.64% and 3.61%, respectively.

Since graphite can fill the voids of the steel fiber skeleton and reduce the void ratio of asphalt concrete, the Marshall stability and splitting strength of remixed asphalt concrete decrease with the increase of steel fiber content, and the Marshall stability and splitting strength of 0.45% graphite and 1.1% steel fiber asphalt concrete are the lowest, at 9.56 kN and 0.93 MPa, which are 13.40% and 12.05% higher than the original asphalt concrete. It shows that the compound graphite/steel fiber conductive asphalt concrete has good mechanical properties. Considering the volume parameters and electrical properties, when the graphite content is 0.68% and the steel fiber content is 0.9–1.1%, the self-sensing asphalt concrete has excellent comprehensive properties.

3.7. Contributions of this study and suggestions for future research

The application of conductive technology in asphalt concrete has been proven to be feasible. However, the majority of previous studies have focused on achieving the best electrical performance. It is not necessary to have particularly outstanding electrical performance to utilize electrical signals for damage sensing in asphalt pavement structures (existing conductive asphalt concrete is not suitable for self-sensing asphalt concrete). This study seeks to develop self-sensing asphalt concrete by incorporating multiple conductive additives. Additionally, the study aims to elucidate the synergistic conductive mechanism of multiphase conductive materials and establish the correlation between the electrical properties of self-sensing asphalt concrete and its pore volume. It is important to note that the current models for the electrical properties and mechanical performance of self-sensing asphalt concrete remain ambiguous both domestically and internationally. Consequently, future research endeavors will be directed toward accurately establishing an electro-mechanical model for self-sensing concrete.

4. Conclusion

In this study, two typical conductive additives, graphite and steel fiber, are used to design a self-sensing asphalt concrete. The design and preparation parameters of graphite and steel fiber conductive asphalt concrete were determined. The volume parameters, electrical properties and mechanical properties of conductive asphalt concrete were comprehensively evaluated, and its conductive mechanism and self-sensing principle were revealed. The main conclusions from this study are as follows:

- (1) Single doped graphite conductive particles penetrate and fill in the asphalt slurry to form a conductive particle chain and form a conductive path, asphalt concrete resistance decreases with the increase of graphite content, the failure distance of conductive particles doped with graphite alone is 2 μm , and the volume content of graphite should not be less than 0.68% to have conductivity.
- (2) The increase of steel fiber in asphalt concrete goes through four stages: (a) non-conductive state without a tunneling network; (b) formation of a conductive network with uniformly dispersed fibers; (c) slight decrease in conductivity due to partial fiber agglomeration; and (d) further increase in electrical conductivity due to stacking or entanglement between agglomerates.
- (3) Composite conductive asphalt concrete benefits from the synergistic effect of steel fiber and graphite (fiber bridging and particle infiltration), with 0.9% steel fiber content amplifying the role of composite graphite.
- (4) A linear relationship exists between the volume parameters (VV) and electrical properties of conductive asphalt concrete within a VV range of 3–6%. However, an exponential relationship emerges when VV exceeds 6%, leading to increased resistivity.
- (5) The compound graphite/steel fiber conductive asphalt concrete, featuring 0.68% graphite content and 0.9% to 1.1% steel fiber content, presents promising comprehensive and electrical properties, positioning it as a potential self-sensing material with strong mechanical characteristics.

Due to the damage to the internal structure of self-sensing asphalt concrete, the conductive path will be reduced, reflecting the deterioration of its electrical performance. In future studies, accurate electrical and mechanical models of self-sensing asphalt concrete can be established to guide the application of self-sensing asphalt concrete.

Funding

This work was supported by the Transportation Technology Project of Department of Transport of Hubei Province (No. 2022–11–1–10), the scientific research fund project of Wuhan Institute of Technology (No. K2021032) and the Pump Priming Award of Liverpool John Moores University.

CRediT authorship contribution statement

Li Yuanyuan: Writing – review & editing, Validation, Software, Methodology, Investigation, Funding acquisition, Conceptualization. **Hu Bowen:** Writing – review & editing, Data curation. **Gao Yangming:** Writing – review & editing, Validation, Software, Methodology, Investigation, Data curation. **Feng Jianlin:** Writing – original draft, Supervision, Data curation. **Kot Patryk:** Writing – review & editing, Formal analysis.

Declaration of Competing Interest

The authors declare that they have no known competing financial interests or personal relationships that could have appeared to influence the work reported in this paper.

Data availability

Data will be made available on request.

References

- H.Y. Chu, J.K. Chen, The experimental study on the correlation of resistivity and damage for conductive concrete, *Cem. Concr. Compos.* 67 (2016) 12–19.
- Y.Y. Li, J.L. Feng, F. Yang, et al., Gradient aging behaviors of asphalt aged by ultraviolet lights with various intensities, *Constr. Build. Mater.* 295 (2021) 123618.
- H. Obaidi, B. Gomez-Meijide, A. Garcia, Induction-Heatable asphalt pellets as a new material in road maintenance, *J. Mater. Civ. Eng.* 30 (11) (2018) 04018300.
- Y. Zhang, M. van de Ven, A. Molenaar, et al., Preventive maintenance of porous asphalt concrete using surface treatment technology, *Mater. Des.* 99 (2016) 262–272.
- S.P. Wu, X.M. Liu, L.T. Mo, et al., Research of self-monitoring mechanism of electrically conductive asphalt-based composite, *Key Eng. Mater.* 326–328 (2006) 1499–1502.
- Y.Q. Bao, Z.Y. Tang, H. Li, Compressive-sensing data reconstruction for structural health monitoring: a machine-learning approach, *Struct. Health Monit.* 19 (1) (2020) 293–304.
- H. Li, J.P. Ou, X.G. Zhang, Xigang Zhang, et al., Research and practice of health monitoring for long-span bridges in the mainland of China, *Smart Struct. Syst.* 15 (3) (2015) 555–576.
- P. Cassese, C. Rainieri, A. Occhiuzzi, Applications of cement-based smart composites to civil structural health monitoring: a review, *Appl. Sci.* 11 (18) (2021) 8530.
- L.J. Meng, L.B. Wang, Y. Hou, et al., A research on low modulus distributed fiber optical sensor for pavement material strain monitoring, *Sensors* 17 (10) (2017) 2386.
- A. Barrias, J.R. Casas, S. Villalba, A review of distributed optical fiber sensors for civil engineering applications, *Sensors* 16 (5) (2016) 748.
- H.S. Park, H.Y. Lee, S.W. Choi, et al., A practical monitoring system for the structural safety of mega-trusses using wireless vibrating wire strain gauges, *Sensors* 13 (12) (2013) 17346–17361.
- Y. Huang, L. Gao, Y.N. Zhao, et al., Highly flexible fabric strain sensor based on graphene nanoplatelet-polyaniline nanocomposites for human gesture recognition, *J. Appl. Polym. Sci.* 134 (39) (2017).
- M. Rasol, F. Schmidt, S. Ientile, et al., Progress and monitoring opportunities of skid resistance in road transport: a critical review and road sensors, *Remote Sens.* 13 (18) (2021) 3729.
- A. Mohan, S. Poobal, Crack detection using image processing: a critical review and analysis, *Alex. Eng. J.* 57 (2) (2018) 787–798.
- Y. Fei, K.C.P. Wang, A. Zhang, et al., Pixel-level cracking detection on 3d asphalt pavement images through deep-learning-based cracknet-v, *IEEE Trans. Intell. Transp. Syst.* 21 (1) (2020) 273–284.
- M. Siahkhoui, G. Razaqpur, N.A. Hoult, et al., Utilization of carbon nanotubes (cnts) in concrete for structural health monitoring (shm) purposes: a review, *Constr. Build. Mater.* 309 (2021) 125137.
- J. Pacheco, B. Savija, E. Schlangen, et al., Assessment of cracks in reinforced concrete by means of electrical resistance and image analysis, *Constr. Build. Mater.* 65 (2014) 417–426.
- H. Siad, M. Lachemi, M. Sahmaran, et al., Advanced engineered cementitious composites with combined self-sensing and self-healing functionalities, *Constr. Build. Mater.* 176 (2018) 313–322.
- M.U. Ahmed, R.A. Tarefder, Incorporation of gpr and fwd into pavement mechanistic-empirical design, *Constr. Build. Mater.* 154 (2017) 1272–1282.
- S. Zhonghe, S. Piet, Electrical conductive behaviour of cementitious composites with low content of hybrid steel-carbon fibre systems, *J. Wuhan. Univ. Technol. (Mater. Sci.)* 13 (1) (1998) 6.
- S.H. Wen, D.D.L. Chung, Effects of carbon black on the thermal, mechanical and electrical properties of pitch-matrix composites, *Carbon* 42 (12–13) (2004) 2393–2397.
- D. Chung, Electrical applications of carbon materials; proceedings of the International conference on carbon; Carbon'02, F, 2002 [C].
- L. Cheng, G. Hao, S. Daquan, et al., Novel conductive wearing course using a graphite, carbon fiber, and epoxy resin mixture for active de-icing of asphalt concrete pavement, *Mater. Struct.* 54 (1) (2021) 48.
- S. Xu, X. Liu, A. Tabakovic, et al., A novel self-healing system: towards a sustainable porous asphalt, *J. Clean. Prod.* 259 (2020) 120815.
- B.S. Huang, X.W. Chen, X. Shu, Effects of electrically conductive additives on laboratory-measured properties of asphalt mixtures, *J. Mater. Civ. Eng.* 21 (10) (2009) 612–617.
- H.P. Wang, J. Yang, H. Liao, et al., Electrical and mechanical properties of asphalt concrete containing conductive fibers and fillers, *Constr. Build. Mater.* 122 (2016) 184–190.
- W.K. Dong, W.G. Li, X.Q. Zhu, et al., Multifunctional cementitious composites with integrated self-sensing and hydrophobic capacities toward smart structural health monitoring, *Cem. Concr. Compos.* 118 (2021) 103962.
- Q.T. Liu, E. Schlangen, A. Garcia, et al., Induction heating of electrically conductive porous asphalt concrete, *Constr. Build. Mater.* 24 (7) (2010) 1207–1213.
- A. Arabzadeh, H. Ceylan, S. Kim, et al., Electrically-conductive asphalt mastic: temperature dependence and heating efficiency, *Mater. Des.* 157 (2018) 303–313.
- X.M. Liu, S.P. Wu, Study on the graphite and carbon fiber modified asphalt concrete, *Constr. Build. Mater.* 25 (4) (2011) 1807–1811.
- S.P. Wu, L.T. Mo, Z.H. Shui, et al., Investigation of the conductivity of asphalt concrete containing conductive fillers, *Carbon* 43 (7) (2005) 1358–1363.
- A. Garcia, E. Schlangen, M. van de Ven, et al., Electrical conductivity of asphalt mortar containing conductive fibers and fillers, *Constr. Build. Mater.* 23 (10) (2009) 3175–3181.
- Q. Liu, E. Schlangen, M. van de Ven, Induction healing of porous asphalt concrete beams on an elastic foundation, *J. Mater. Civ. Eng.* 25 (7) (2013) 880–885.
- X.M. Liu, S.P. Wu, Research on the conductive asphalt concrete's piezoresistivity effect and its mechanism, *Constr. Build. Mater.* 23 (8) (2009) 2752–2756.
- X.M. Liu, S.P. Wu, Study on the Piezoresistivity Character of Electrically Conductive Asphalt Concrete; proceedings of the International Conference on Chemical Engineering and Advanced Materials, Changsha, PEOPLES R CHINA, F May 28–30, 2011 [C]. 2011.
- A. Menozzi, A. Garcia, M.N. Partl, et al., Induction healing of fatigue damage in asphalt test samples, *Constr. Build. Mater.* 74 (2015) 162–168.
- Q.T. Liu, W. Yu, S.P. Wu, et al., A comparative study of the induction healing behaviors of hot and warm mix asphalt, *Constr. Build. Mater.* 144 (2017) 663–670.
- P. Park, Characteristics and applications of high-properties fiber reinforced asphalt concrete (D), University of Michigan, 2012.
- Y. Rew, A. Baranikumar, A.V. Tamashauskay, et al., Electrical and mechanical properties of asphaltic composites containing carbon based fillers, *Constr. Build. Mater.* 135 (2017) 394–404.
- S. Xu, Self-Healing Porous Asphalt: A Combination of Encapsulated Rejuvenator and Induction Heating, Delft University of Technology, 2020.
- S. Xu, A. Garcia, J.F. Su, et al., Self-Healing asphalt review: from idea to practice, *Adv. Mater. Interfaces* 5 (17) (2018) 1800536.
- Z. Chen, R.N. Liu, P.W. Hao, et al., Developments of conductive materials and characteristics on asphalt concrete: a review, *J. Test. Eval.* 48 (3) (2020) 20190179.
- F. Chen, R. Balieu, A state-of-the-art review of intrinsic and enhanced electrical properties of asphalt materials: theories, analyses and applications, *Mater. & Des.* 195 (2020) 109067.
- P. Pan, S.P. Wu, F.P. Xiao, et al., Conductive asphalt concrete: a review on structure design, performance, and practical applications, *J. Intell. Mater. Syst. Struct.* 26 (7) (2015) 755–769.
- S. Ullah, S.H. Wan, C. Yang, et al., Self-stress and deformation sensing of electrically conductive asphalt concrete incorporating carbon fiber and iron tailings, *Struct. Control Health Monit.* 29 (9) (2022) [2023–11–25].
- M. Messaoud, B. Glaoui, O. Abdelkhalik, The effect of adding steel fibers and graphite on mechanical and electrical behaviors of asphalt concrete, *Civ. Eng. J.* 8 (2) (2022) 348–361.
- J.D. Ren, C. Xing, Y.Q. Tan, et al., Void distribution in zeolite warm mix asphalt mixture based on x-ray computed tomography, *Materials* 12 (12) (2019) 1888.
- Q.T. Xu, D.D. Zhao, F.Q. Zhang, Study on damage of the OGFC mixture based on characteristics of void distribution, *Adv. Mater. Sci. Eng.* 2022 (2022) 1–10.
- A.Q. Chen, G.D. Airey, N. Thom, et al., Characterisation of fatigue damage in asphalt mixtures using x-ray computed tomography, *Road. Mater. Pavement Des.* 24 (3) (2023) 653–671.
- X.M. Liu, S.P. Wu, X.L. Yang, Smart characteristics of conductive asphalt concrete [J]. Zhongnan Daxue Xuebao (Ziran Kexue Ban) (/), J. Cent. South Univ. (Sci. Technol.) 40 (2009) 1465–1470.

- [51] J. Zhang, Z. Liang, T. Hreid, et al., Fabrication and investigation of a new copper-doped screen-printable carbon paste's conductive mechanism by AFM, *RSC Adv.* 2 (11) (2012) 4787.
- [52] Z. Li, X. Liu, Y. Lian, et al., The percolation mechanism of surfactant-free microemulsions witnessed by the conductivity measurement, *World J. Eng.* 13 (2) (2016) 142–148.
- [53] K.S. M C D, V. Antara, A. Vaidyanathan, et al., Comparison of electrochemical response and electric field emission characteristics of pristine La₂NiO₄ and La₂NiO₄/CNT composites: origin of multi-functionality with theoretical penetration by density functional theory, *Electrochim. Acta* 369 (2021) 137676.